



13th World Conference on Earthquake Engineering
Vancouver, B.C., Canada
August 1-6, 2004
Paper No. 1559

EXPERIMENTAL STUDY ON SEISMIC RESTORING PERFORMANCE OF REINFORCED CONCRETE SHEAR WALLS

Hong-nan LI¹ and Bing LI²

SUMMARY

Quasi-static test of nine reinforced concrete shear walls are carried out under cyclic lateral loading. The relationship between force and displacement is obtained so that the macro-finite element model for R/C shear wall presented in the paper is verified. The corresponding formulations for this model are given. Through comparing the destructed behaviors and grades of the walls under different axial compression ratio and shear span ratio based on the analysis of test and hysteretic curve, it can be concluded as: with the increasing of axial compression ratio to some range, the bearing capacity of shear wall will increase if the shear span ratio of shear walls are same, but the ductility of walls will descend, and degradation of strength and stiffness are also more serious. At the same time, with the increasing of shear span ratio, the destructed behavior of shear walls will be transited from shear wreck to bend wreck. The bearing capacity will fall, while the ductility and capability of consuming energy of shear walls will be strengthen.

INTRODUCTION

A realistic and practical prediction of the inelastic response of reinforced concrete (R/C) frame-wall structures under seismic loads requires analytical models that are both capable of reproducing the nonlinear response of each structural component with reasonable accuracy and simplicity enough to allow economically numerical solutions [1]. The reliability of a frame-wall model depends on the accuracy in describing the hysteretic behavior of structural members and their interaction. In particular, the use of a suitable wall model is considered crucial. Therefore, nowadays the inelastically analytical model of shear walls in reinforced concrete structures can be made either using a microscopic finite element approach or a macroscopic finite element approach [2].

At present, macroscopic finite unit models of R/C shear wall in references mainly include the equivalent beam and truss model, three-vertical-line-element model, multiple-vertical-line-element model, four-spring models, shear panel model and so on [3-14]. The main drawback of a beam model is that rotations occur around the central axis of shear wall when the wall is horizontally loaded. Thus, the important phenomena observed (i.e., fluctuation of the neutral axis in the cross-section area) in

¹ Professor, Dalian University of Technology, Dalian, China. Email: hnli@dlut.edu.cn

²PHD student, Dalian University of Technology, Dalian, China. Instructor, Shenyang Architecture and Civil Engineering Institute, Shenyang, China, Email: Bingleesy@sohu.com

experiments are disregarded and consequent effects in a frame-wall structure (i.e., the outrigger interaction with frames surrounding the wall) are not taken into account adequately. The truss model is generally available for monotonic loading because of difficulties in defining structural topology and properties of the truss elements under cyclic loading [3].

Based on experimental results of a full-scale model of a seven-story R/C building, Kabeyasawa et al. [4] presented a three-vertical-line-element model for the shear wall. The model, although relatively simple, incorporates the main features of the experimentally observed behavior, which the equivalent beam model fails to describe. It idealizes a generic wall member as three vertical line elements with infinitely rigid beams at the top and bottom floor, in which two outside elements represent the boundary columns of wall, while the central element stands for a one-component wall model with vertical, horizontal and rotational springs concentrated at the base. The finite rigid element with a certain length could be placed between the spring assembly and the lower rigid beam. Such a wall model was intended to simulate the deformation of the wall member with uniformly distributed curvature. And this model can simulate the migration of the neutral axis of the wall cross-section. However, many of the assumptions for the model are empirical and even seem to be arbitrary such as the stiffness properties of the rotational spring [5].

The multiple-vertical-line-element model was presented by Azzato and Vulcano[6,7] based on the three-vertical-line-element model. The central elements of this model were transferred by paratactic springs and the numbers of springs may be chosen according to different accuracy [8]. In order to limit the empirical assumptions as few as possible, they replaced the hysteretic model of axial stiffness with the two-axial-element-in-series model to simulate the response of the truss elements, while the assumption of even cross-section was broken [9]. For the rotative center of wall, Vulcano et al. defined the parameter, $c=0.4$, through the method by trial and error, and Sun et al. [10] determined c to be equal to 0.5 based on Timoshenko layer-beam element.

Another improved model is the four-spring model offered by Linda et al [11]. The rotative spring in the three-vertical-line-element model was neglected and the rotation of the wall was controlled by outside springs. However, four-spring model adopted several coefficients, and some of them were obtained from tests falling in the range of 0.2-0.8. This is a relatively large scope which may cause the results to be uncertain. Hence, it is desirable to narrow the range of the parameters in future studies.

Milev [12] and Colotti [13] developed the shear panel model respectively. The model is the combination of macroscopic finite element and microscopic finite element methods, in which the vertical, horizontal and rotational springs in the center of the three-vertical-line-element model were replaced by a two-dimensional panel, and the panel was analyzed by the microscopic finite element method. Although this method improves the result precision, the computational time increases at the same time [14].

In general, the most suitable model could be the multiple-vertical-line-element model in the authors' opinion of this paper [15-16]. Nevertheless, the changes of shear stiffness and axial stiffness in this model are considered respectively, which should be coupled in fact. Therefore, this aspect needs to be improved [17].

This paper provides new test data pertaining to the seismic behavior of R/C shear wall. Nine shear wall specimens are tested with the combined constant axial loads and cyclically reversed loads[18]. The concrete strength is 30 MPa in the experiments. The influences of two parameters are investigated: 1) the axial compression ratio; 2) the shear-span ratio. Through compared with tests, a new macroscopic finite element model for R/C shear wall is presented and some significant conclusions are drawn for practical engineering application.

EXPERIMENTAL PROGRAM

Test Specimens

According to the Chinese Code for Design of Concrete Structures[18], nine R/C shear walls were designed for the experimental investigation. The cross section size of specimen is 700mm×100mm. In order to change the shear-span ratio from 1.0-2.0, the specimens were manufactured with different heights, 700 mm, 1050 mm and 1400 mm, respectively, and each has three wall specimens. To meet the need of flexural and ductile features, the wall was designed with boundary columns at two sides. Four steel bars with 12 mm in diameter were placed in each column, in which the distributed steel tie is 6.5 mm in diameter and the distance between them is 150mm. Six distributed steel bars with 6.5 mm in diameter were vertically placed in the walls. Based on different heights of the specimens, sixteen (h=1400mm), twelve (h=1050mm) and eight (h=700mm) 6.5-mm-diameter steel bars were horizontally placed, respectively (Fig.1).

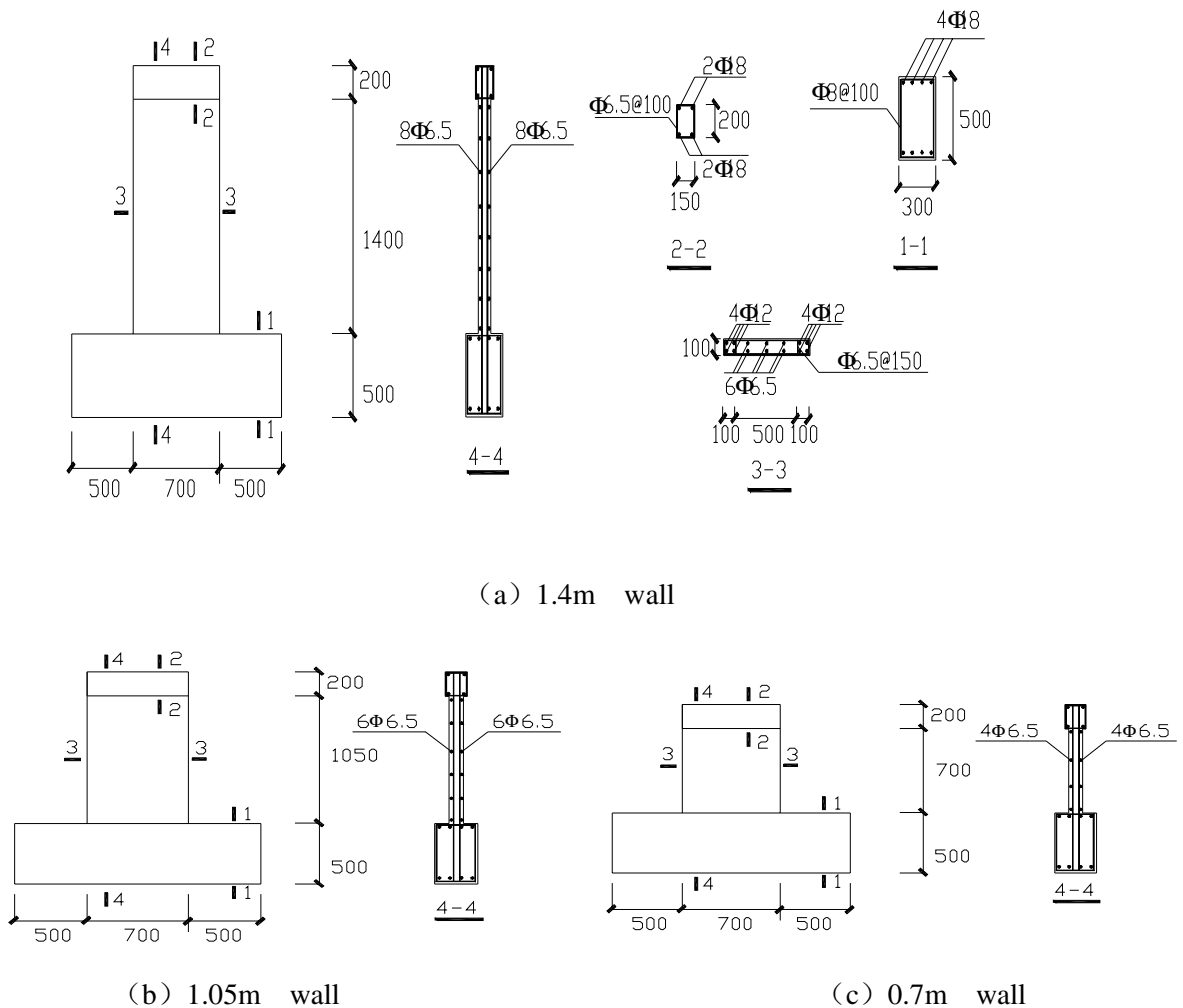
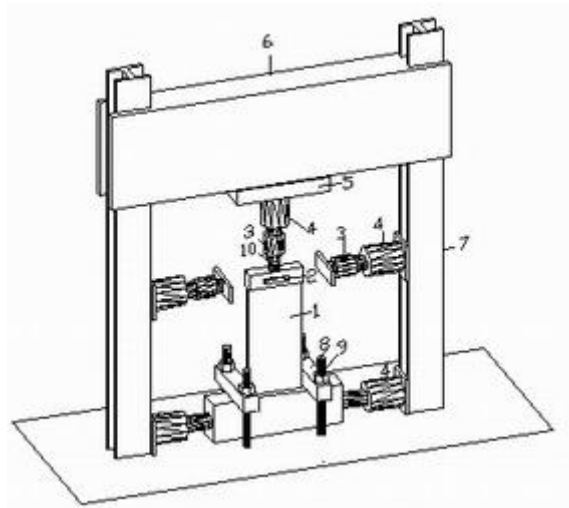


Fig.1 Dimensions of Walls and Position of Reinforcement

Testing Setup

The wall specimens were tested in a steel frame shown in Fig.2 and 3 [20-23]. The horizontal load was applied by two 1000KN hydraulic jacks and was controlled by the loading transducers connected with the jacks. Two ball joints were installed for the stabilization of horizontal load. The axially compressive forces on the wall were provided by a 1000KN hydraulic jack connected with the loading transducer and ball joint. The slip thick plate (Fig.2) was fixed between the crossbeam and jack in order to make the vertical load always at the midpoint of the wall.

The displacement transducer was placed at the midpoint of top of specimen and it and loading transducers were connected with signal magnifier linked to UCAM data acquisition system. The strain of each steel bar was measured by strain gages that were also connected with UCAM device. At last the data of experiments were processed by a computer.



- | | | |
|-------------|----------------------------|--------------------|
| 1. specimen | 2. displacement transducer | 3. load transducer |
| 4. jack | 5. slip thick plate | 6. crossbeam |
| 7. column | 8. beam | 9. bolt |
| | | 10. joint |

Fig. 2 Experimental Setup



Fig. 3 Photograph of Experimental Setup

The test began with the application of the axial load at the targeted values listed in table 1. For the cycle of horizontal load, the force levels were controlled at initial stage until the horizontal force reached the

yielding load. After the point, each cycle loading period was applied under displacement control with a maximum displacement equal to 1, 2, 3, ..., n times of the measured yielding displacement up to specimen failure. At last the test ended when ultimate load dropped to 85% of the maximum bearing capacity.

Table 1 Parameters of Specimens for Test

Number	Grade of concrete	Ratio of steel bars to columns boundary	Ratio of vertical steel bars to wall	Ratio of horizontal steel bars to wall	Vertical load N (KN)
Wall-1	C30	4.5%	0.4%	0.37%	100
Wall-2	C30	4.5%	0.4%	0.37%	200
Wall-3	C30	4.5%	0.4%	0.37%	300
Wall-4	C30	4.5%	0.4%	0.37%	100
Wall-5	C30	4.5%	0.4%	0.37%	200
Wall-6	C30	4.5%	0.4%	0.37%	300
Wall-7	C30	4.5%	0.4%	0.37%	100
Wall-8	C30	4.5%	0.4%	0.37%	200
Wall-9	C30	4.5%	0.4%	0.37%	300

RESULTS AND ANALYSES OF TESTS

Failure and Analysis of Walls

1) For the specimens of which shear span ratio was 1.0 (Wall-1, Wall-2 and Wall-3), the processes of failure show as follows:

The specimen Wall-1 with the axial compression ratio, 0.1, was within elastic range before the concrete cracked. And then when the horizontal loading was enhanced to 70 KN, an oblique crack firstly appeared on the ventral wall. With the increase of loading, the several oblique cracks appeared and gradually augmented, and at the same time horizontal cracks also appeared on the boundary columns. In the stage, although the ventral wall body was divided into several net blocks, the bearing capacity of the specimen might still be increased because the mid-body of the wall among the homo-tropic cracks could support the pressure and the tensile force can be supported by steel bars in the wall. At this time, the specimen had the less tip displacement and the less width of cracks. And in the loading stage by controlling displacement, with the increasing of tip displacement, the concrete at diagonal direction in ventral wall body, under the united action of shear and compressive forces, arrived at the ultimate strength and then crumbled. The behavior of specimen showed the obvious fragility and belonged to shear failure.

For the specimens Wall-2 and Wall-3, the failure behaviors resembled Wall-1. The cracking load and ultimate load enhanced with the increasing of axial compression ratio. And there is a lack of distinct yielding points for the three specimens.

2) For the specimens of which shear span ratio was 1.5 (Wall-4, Wall-5 and Wall-6), the processes of failure are as follows:

For the specimen Wall-4 with the axial compression ratio, 0.1, the hysteretic curve was almost a linear when the horizontal load was less than 40KN. While increasing the load to 50KN, the concrete of the ventral wall began to crack, and then the horizontal cracks appeared on the boundary columns. At the time that the horizontal force was enhanced to 70 KN, the oblique cracks appeared on the mid-wall body.

With the increasing of load, the oblique cracks also became wider and gradually came to the neutral axis. And finally the critical crack appeared. After the lateral load exceeded 130KN, the width of the declined crack quickly increased and the horizontal bars cross the cracks yielded. Later, the pattern of applying loading by controlling the displacement began to be used. During this stage, the degradation of stiffness occurred and the curves of force-displacement showed the well ductility with the increase of loading. And the specimens still could undertake a certain load. Meanwhile, the strength redeemed obviously in some content when the external force was unloaded. From the Figure 4, it can be seen that the ductility of specimen exhibited quite well. The destructive classifications of the three walls all belong to the shear-bending mode.

The trait of destroys of the specimens, Wall-5 and Wall-6, also resembled with Wall-4. And with the increasing of axial compression ratio, the cracking and ultimate loads all enhanced and there were relatively obvious yielding points for the three specimens.

3) For the specimens of which shear span ratio was 2.0 (Wall-7, Wall-8 and Wall-9), the processes of failure are as follows:

For the specimen, Wall-7, with the axial compression ratio, 0.1, when the horizontal load was less than 30KN, loading was controlled and the hysteretic curve was almost a straight line. During the period the concrete did not crack. Increasing the force to 30KN, the flexural cracks appeared on the tension area. At the same time, the stiffness of the specimen altered. When the horizontal force was enhanced to 70 KN, the oblique cracks became wider and moved gradually to the neutral axis. Within the stage of displacement control, the characteristics of fine ductility and capability of consuming energy were exhibited also. Thus, the destructive modes of the three wall specimens all belong to bending failure.

Analogously, the cracking loads, yielding points and ultimate loads for the specimens, Wall-8 and Wall-9, also enhanced with the increase of axial compression ratio.

Through comparing the failing modes of different shear span ratios, it can be concluded as follows:

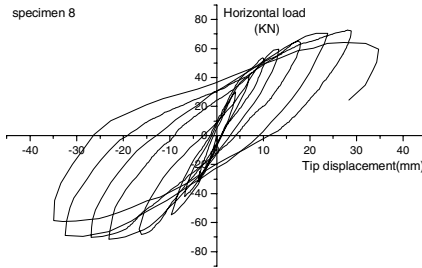
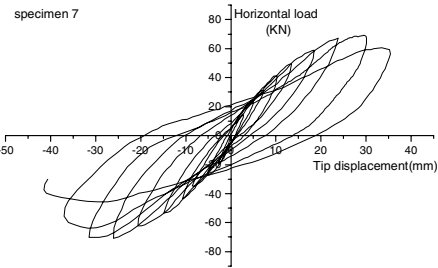
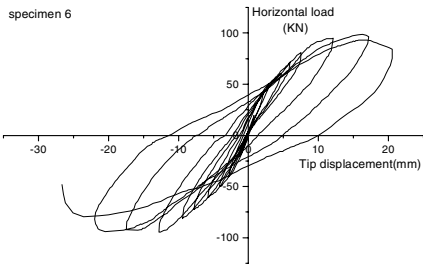
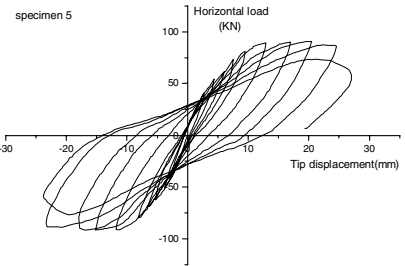
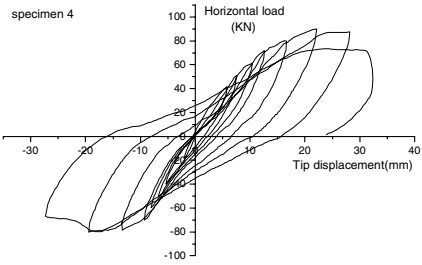
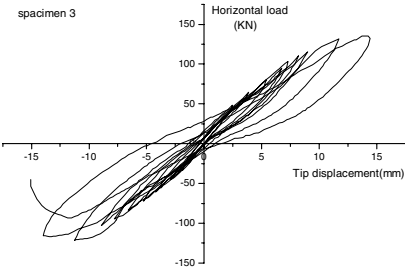
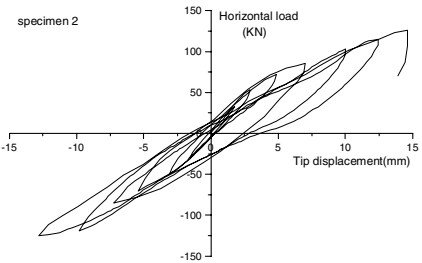
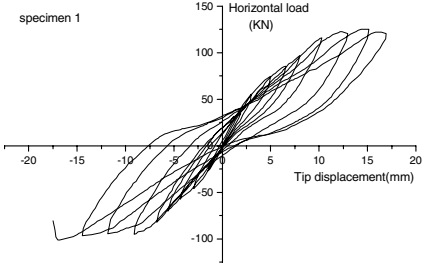
For the wall specimens with the shear span ratio, 1.0, they were typical shear failure because the diagonal shear cracks were quite obvious. When the shear span ratio was 1.5, not only were the diagonal shear cracks of walls obvious, but also the flexural cracks appeared and the concrete at the bottom of boundary columns was crushed so that they showed the combined shear and bending failing mode. And for the third types of specimens with the shear span ratio, 2.0, the diagonal shear cracks were inconspicuous, while the flexural cracks were visible and the concrete at the bottom of the columns was smashed. Hence, they displayed the flexural failing mode.

Hysteretic Characteristics

Fig 4 shows the hysteretic curves of relations between the lateral loads and displacements of nine wall specimens.

1) For the specimens Wall-1, Wall-2 and Wall-3 with the small shear span ratio, the hysteretic curves showed approximately linear before cracks emerged and the stiffness of specimens decreased with the developing of the cracks. Later on, the cycle curves displayed arc shape along with the increasing of external loads. However, the yielding points of the wall specimens were not distinct and they failed with a sudden pattern. Therefore, it was typically brittle failure.

With the increase of axial compression ratio, compared with specimen Wall-1, specimen Wall-2 had 14% and 1.3 enhancements for the cracking load and original stiffness respectively, while a 14% decrease for the ultimate displacement. And for the specimen Wall-3, there were 28% and 1.5% improvements for the cracking load and original stiffness respectively, and a 16% abatement of the ultimate displacement.



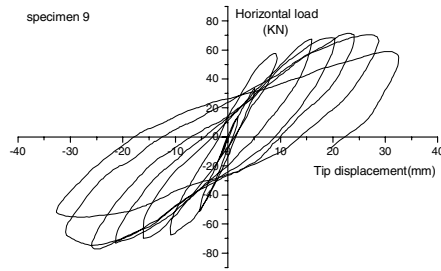


Fig. 4 Tested Hysteretic Curves of Uncorrected Lateral Load versus Displacement

2) For the specimens Wall-4, Wall-5 and Wall-6 with the medium shear span ratio, cracking points of the hysteretic curves were not clear, while the yielding points were visible. Moreover the descending phases of the curves were distinct. As shown in Fig.5, these three pieces of walls had better ductility and more cyclic times for hysteretic curves than the walls that were with the smaller shear span ratio.

Along with the increase of axial compression ratio, specimen Wall-5 had 1.6% and 11% enhancements for the ultimate load and original stiffness respectively, while a 15.6% decrease for the ultimate displacement. And for the specimen Wall-6, compared with specimen Wall-4, there were 14% and 6.7% enlargements for the cracking load and ultimate load, a 21% augment for the original stiffness and a 22% abatement for the ultimate displacement.

3) For the specimens Wall-7, Wall-8 and Wall-9 with the larger shear span ratio, the hysteretic curves of these walls revealed clear cracking points, yielding points and the descending stage. The three pieces of walls displayed best ductility and most cyclic times in all types of wall specimens with different axial compression ratios.

With the improvement of axial compression ratio, compared with specimen Wall-7, specimen Wall-8 had 2.2% and 6% enhancements for the ultimate load and original stiffness, a 1.3% decrease for the ultimate displacement; and the specimen Wall-9 gained 33% and 6% increases for the cracking load and ultimate load, and a 23% addition for the original stiffness and a 8% abatement for the ultimate displacement, respectively.

The results of the test were shown in table 2.

Table 2 The Results of the Test

Number	Shear span ratio	Axial compression ratio	Crack load (KN)	Ultimate load (KN)	Ultimate displacement (mm)	Original stiffness (KN/mm)
Wall-1	1	0.1	70	120.35	16.96	18.01
Wall-2	1	0.2	80	125.44	14.63	18.26
Wall-3	1	0.3	90	134.96	14.27	18.29
Wall-4	1.5	0.1	50	87.15	28.20	13.49
Wall-5	1.5	0.2	50	88.62	23.80	14.99
Wall-6	1.5	0.3	60	92.94	21.98	16.35
Wall-7	2	0.1	30	70.40	35.45	7.50
Wall-8	2	0.2	30	71.96	34.97	7.95
Wall-9	2	0.3	40	74.67	32.63	9.23

MACRO-FINITE ELEMENT MODEL FOR SHEAR WALL

In the nonlinear analysis and design of shear wall, failing mode is normally assumed for bending failure and modeled with the multiple-vertical-line-element model. In the model, the axial springs firstly reached the nonlinear state and then the shear springs did. Thus, the effect of axial stiffness on shear stiffness was neglected. In fact, the change of axial stiffness must arouse the change of shear stiffness. Therefore, the authors in this paper combine the effects of axial stiffness and shear stiffness to propose the more rational multi-component-in-parallel model as follows (Fig. 5), in which the variety of shear stiffness is along with the axial stiffness:

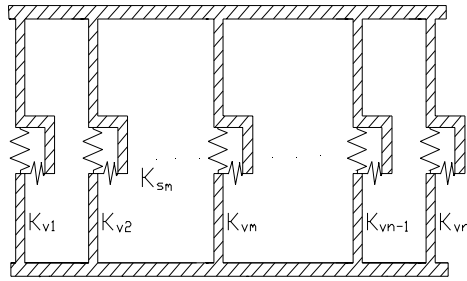


Fig.5 Proposed Macro-Finite Element Model

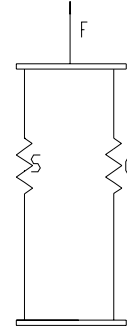


Fig.6 Axial Spring Model

1) For the axial stiffness of each vertical spring, the two parallel components C and S (Fig.6) represent the mechanical behaviors of the concrete and steel, respectively, and different hysteretic models (Fig.7 and 8) were adopted to simulate the different characteristics of materials.

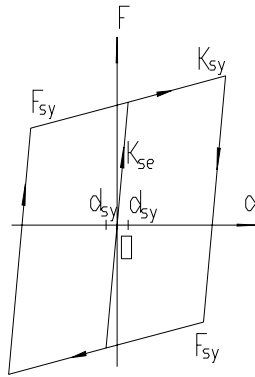


Fig. 7 Hysteretic Model of Steel Bar

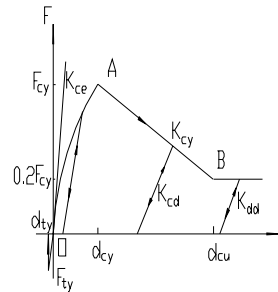


Fig. 8 Hysteretic Model of Concrete

2) It is assumed that the axial deformation of vertical element is u and its original shear stiffness is K_e . The stiffness of each shear spring is determined by the different state of vertical spring as follows:

① When the vertical spring undertakes the compressive force, its axial deformation is expressed by d_{sy} as the steel bar in the vertical elements yields; and its axial deformation is expressed by d_{cy} as the concrete in the vertical elements reaches the peak strain (where the peak compressive strain is 0.0033). Thus, the stiffness of the vertical spring is determined by:

A. When $u \leq d_{sy}$, if the steel bar dose not attain to yielding point, the elastic shear stiffness is K_e ; if the steel bar yields, while the concrete dose not reach the peak strain, the shear stiffness is given by $r_1 \cdot K_e$; and if the concrete also arrives at the peak strain at the same time, the stiffness is $r_2 \cdot K_e$, where $r_1 = 0.5$ and $r_2 = 0.02$ are obtained based on the above test results.

B. When $d_{sy} < u \leq d_{cy}$, if the concrete dose not attain to the peak strain, the shear stiffness can be drawn through the interpolation between $r_1 \cdot K_e$ and $r_2 \cdot K_e$ according to the axial deformation as follows:

$$K = r_1 \cdot K_e + \frac{u - d_{sy}}{d_{cy} - d_{sy}} \cdot (r_2 - r_1) \cdot K_e \quad (1)$$

If the concrete passes the peak strain, the shear stiffness is $r_2 \cdot K_e$.

C. When $u > d_{cy}$, the shear stiffness takes $r_2 \cdot K_e$.

②When the vertical spring suffers from the tensile force, if the first crack on the wall specimen appears, the axial deformation of the vertical element is expressed by d_{ty} ; if the steel bar reaches yielding point, the axial deformation of the vertical element is expressed by d_{sy} ; and if the steel bar in the vertical element reaches the peak strain, its axial deformation is replaced by d_{su} and then the stiffness of vertical spring can be determined as follows:

A. When $u \leq d_{ty}$, if the crack dose not appear, the elastic shear stiffness is K_e ; if the concrete has cracked, but steel bar dose not yield, the shear stiffness may be replaced by $r_3 \cdot K_e$; if the steel bar has passed the yielding point and dose not reach the peak strain, the shear stiffness is represented by $r_4 \cdot K_e$, and if the steel bar attains to strain, then the shear stiffness the peak is given by $r_5 \cdot K_e$, where $r_3 = 0.5$, $r_4 = 0.15$ and $r_5 = 0.02$ are obtained based on the above test results..

B. When $d_{ty} < u \leq d_{sy}$, if the steel bar dose not yield, the shear stiffness can be drawn through interpolation between $r_3 \cdot K_e$ and $r_4 \cdot K_e$ according to the axial deformation by

$$K = r_3 \cdot K_e + \frac{u - d_{ty}}{d_{sy} - d_{ty}} \cdot (r_4 - r_3) \cdot K_e \quad (2)$$

If the steel bar has passed the yielding point and dose not reach the peak strain, the shear stiffness is expressed by $r_4 \cdot K_e$; if it has attained to peak strain, the shear stiffness takes $r_5 \cdot K_e$.

C. When $d_{sy} < u \leq d_{su}$, if the strain of steel bar is less than the peak one, the shear stiffness can be drawn through interpolation between $r_4 \cdot K_e$ and $r_5 \cdot K_e$ given by

$$K = r_4 \cdot K_e + \frac{u - d_{sy}}{d_{su} - d_{sy}} \cdot (r_5 - r_4) \cdot K_e \quad (3)$$

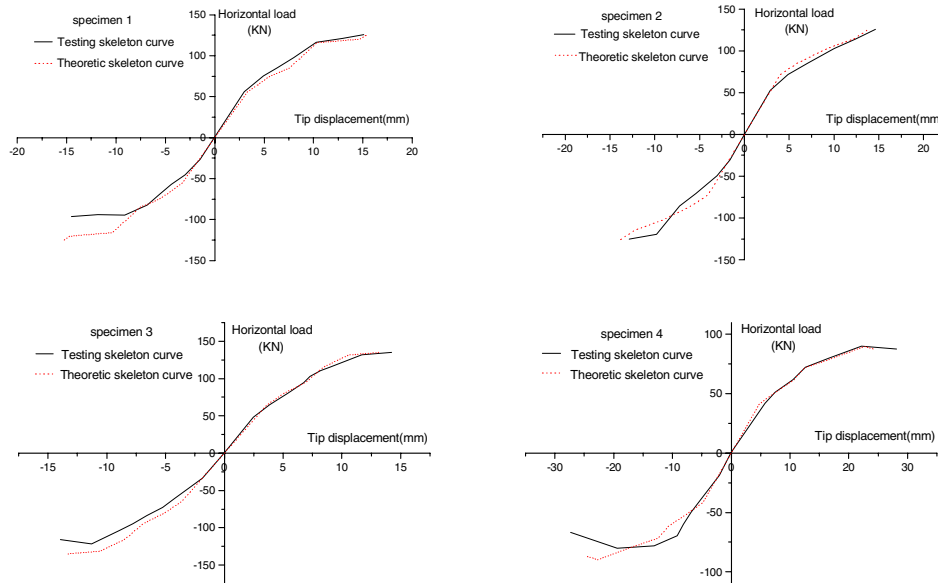
If the steel bar has reached the peak strain, the shear stiffness takes $r_5 \cdot K_e$.

D. When $u > d_{su}$, the shear stiffness is expressed by $r_5 \cdot K_e$.

③ The shear stiffness of the wall can be obtained by combination with all vertical springs.

VERIFICATION OF PROPOSED MODEL

In order to confirm the macro-finite element model presented in this paper, the comparisons are made with results of experiments and the nonlinear analysis based on the above model for the test specimens as shown in Fig. 9. It can be seen from the contrasted figures that the curves of tests and theoretical models agree quite well with each other.



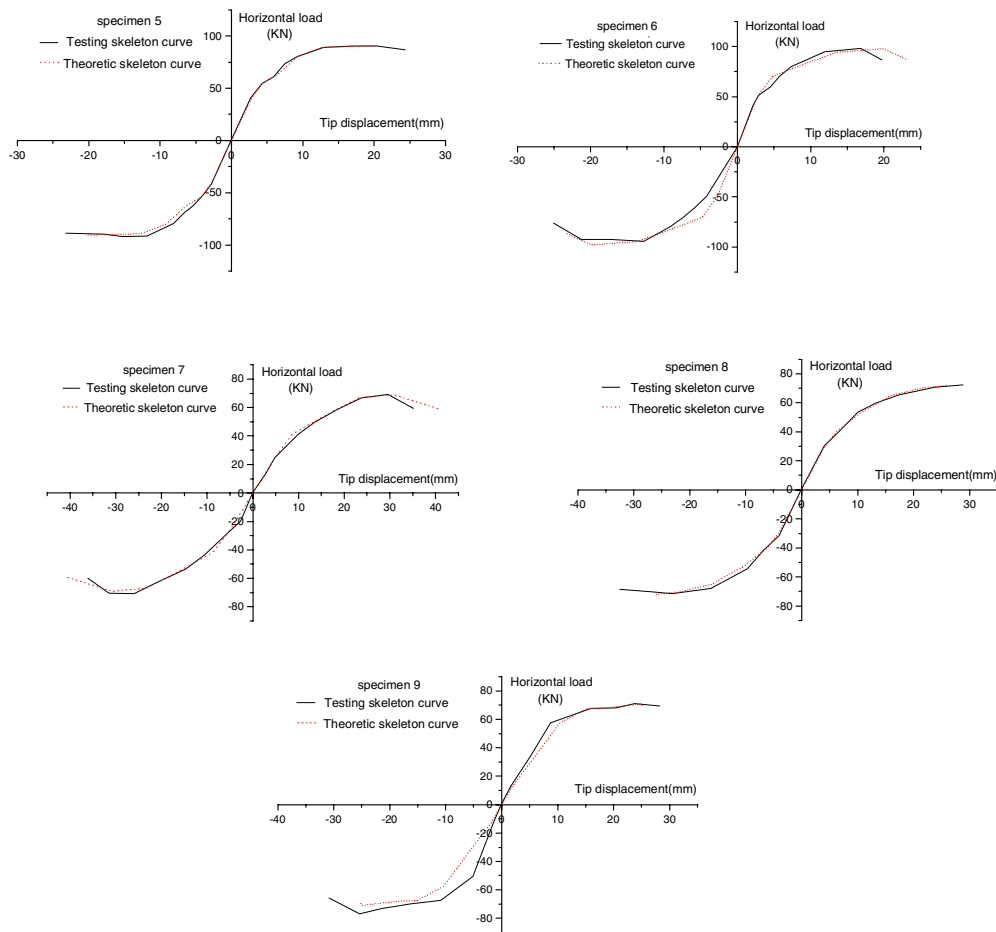


Fig.9 Comparisons with Tested and Theoretic Skeleton Curves

CONCLUDING REMARKS

Based on the above experimental and analytical results, some conclusions with engineering significance can be drawn as follows:

- (1) With the increase of axial compression ratio to some range, the bearing capacity of shear wall will increase if the shear span ratio of walls is the same, while the ductility will descend and degradations of strength and stiffness are also more serious.
- (2) The shear span ratio is an important factor for the disruptive form of shear wall. If other parameters are the same, the destructed behavior of shear walls will be changed from the shear failure to bending failure with the enhancement of shear span ratio. And the bearing capacity will fall, while the ductility and capability of consuming energy will be strengthened.
- (3) Through combing the shear and axial stiffness with a few springs, the macro-finite element model for R/C shear wall presented here is rational with the experimental verifications.

ACKNOWLEDGMENTS

This project is supported by the National Natural Science Foundation of China under grant No. 50025823. This support is greatly appreciated.

REFERENCES

- [1] Vincenzo Colitti, “ Shear behavior of RC structure walls”, Journal of Structural Engineering, Vol.119, NO.3, March, 728-746, 1993.
- [2] J. Fu, A. Shibata, J.-i. Shibuya and T. Saito, “ 3-D inelastic earthquake response of RC frames with shear walls”, Proc. Of the Tenth world Conference on Earthquake Engineering,1992: 4303-4308
- [3] A.Vulcano, “ Use of wall macroscopic models in the nonlinear analysis of RC frame-wall”, Earthquake Engineering, Tenth World Conference, 4309-4312, 1992 Balkema, Rotterdam
- [4] Kabeyaawa T et al. U.S.-Japan cooperative research on R/C full-scale building test, Part 5:Discussion of dynamic response system[A]. Proc. 8th of WCEE[c].627-634.
- [5]A.Vulcano, V.V.Bertero, “ Analytical models for predicting the lateral response of RC shear walls: evaluation of their reliability”,Report UCB/EERC-89/19, Univ. of California, Berkeley, 1987.
- [6]F.Azzato, A.Vulcano, “ Modeling of RC frame-wall structures for nonlinear seismic analysis”, Eleventh world conference earthquake engineering,paper No.1411,1996.
- [7]A.Vulcano,V.V.Bertero and V.Colotti, “ Analytical modeling of R/C structure walls”, Ninth world conference on earthquake engineering, August 2-9,1988,Vol.VI:41-46.
- [8] Li Guoqiang, Zhou Xiangming, Ding Xiang, “ Models of reinforced concrete shear walls for nonlinear dynamic analysis”. World information on earthquake engineering, Vol.16,No.2, 13-18,2000.
- [9]Jiang Jinren, Li Xiaodong, “ State-of-art of nonlinear seismic response analysis for R/C frame-wall structure”, World Information on Earthquake Engineering, Vol.13,No.2, Jun.,1997:30-35
- [10]Sun Jingjian, “ Review of models for nonlinear analysis of R/C shear wall”, World Information on Earthquake Engineering, No.1, 1994:43-46
- [11]P.Linde, H.Bachmann, “ Dynamic modeling and design of earthquake-resistant walls”, Earthquake engineering and structural dynamics, Vol.23, 1331-1350, 1994
- [12]Milev J I. Two dimensional analytical model of reinforce concrete shear walls[A]. Proc. of 11th WCEE[C],1996.
- [13] Colotti, V., “ Shear Behavior of R/C Structural Walls”, J.Struct.Engrg. 1993,119(3).
- [14]Wang Haibo, Wang Mengfu, Shen Pusheng, “ Nonlinear analysis of seismic responses for shear wall structure with opening holes”, Engineering aseismic,No.3,2000:3-6.
- [15]Jiang Huanjun, Lⁱⁱ Xilin, “ Research on application of macroscopic shear wall model”, Earthquake engineering and engineering vibration,Vol.23,No.1,Feb.,2003:38-43.
- [16]Jiang Huanjun, Lⁱⁱ Xilin, “ Analysis of shear wall structures using a type of wall element”, Earthquake engineering and engineering vibration,Vol.18,No.3,Sep.,1998:40-48.
- [17]Li Bing, Li Hong-nan, “ Analysis of macroscopic finite unit models for R/C shear wall”, Journal of southeast university, Vol.32 Sup. Sept.2002:291-294.
- [18]Chinese code for design of concrete structures GBJ50010-2002. 189-197
- [19]Li Hongnan, Wang Qiang, LiBing, “ Experiment on characteristics of Multi-dimensional restoring forces of reinforced concrete frame columns”, Journal of southeast university(natural science edition),Vol.32, No.5, Sept.2002
- [20]Frederic Legeron and Patrick Paultre, “ Behavior of high-strength concrete columns under cyclic flexure and constant axial load”, ACI Structural Journal,V.97,No.4,July-August 2000: 591-601
- [21]Miha Tomazevic,Marjana Lutman,and Ljubo Petkovic, “ Seismic behavior of masonry walls:Experimental simulation”, Journal of structural engineering, Vol.122,No.9,September, 1996: 1040-1047

- [22]D.Lefas, D. Kotsovos and N.Ambraseys, “ Behavior of reinforced concrete structural walls: strength, deformation characteristics,and failure mechanism”, ACI structure journal,V.87,No.1,1990: 23-31.
- [23]S.T.Mau and T.T.C.Hsu, “ Shear behavior of reinforced concrete framed wall panels with vertical loads”, ACI Structural journal, May-June,1987:228-234.